

# Human umbilical cord perivascular cells (HUCPVC)

## A mesenchymal cell source for dermal wound healing

Nazlee Zebardast,<sup>1</sup> David Lickorish<sup>1</sup> and John E. Davies<sup>1,2,\*</sup>

<sup>1</sup>Institute of Biomaterials and Biomedical Engineering; <sup>2</sup>Faculty of Dentistry; University of Toronto; Toronto, ON Canada

**Key words:** human umbilical cord perivascular cells, HUCPVC, dermal wound healing, Balb/c mice, PKH67, Ki67, wound tensile strength, MSC

**Abbreviations:** MSC, mesenchymal stem cell; hBM-MSC, human bone marrow-derived MSC; HUCPVC, human umbilical cord perivascular cell; ECM, extracellular matrix; WTS, wound tensile strength

Human bone marrow mesenchymal stem cells (hBM-MSC) have recently been employed in the clinical treatment of challenging skin defects. We have described an MSC population that can be easily harvested from human umbilical cord perivascular tissue, human umbilical cord perivascular cells (HUCPVC), which exhibit a higher proliferative rate and frequency than hBM-MSC. Our objective was to establish whether HUCPVC could promote healing of full thickness murine skin defects, and thus find utility as a cell source for dermal repair. To this end, bilateral full thickness defects were created on the dorsum of Balb/c nude mice. Fibrin was used as a delivery vehicle for  $1 \times 10^6$  PKH67-labeled HUCPVC with contralateral controls receiving fibrin only. Epifluorescent and brightfield microscopic evaluation of the wound site was carried out at 3 and 7 days while mechanical testing of wounds was carried out at 3, 7 and 10 days. Our results show that by 3 days, marked contraction of the wound was observed in the fibrin controls whilst the HUCPVC samples exhibited neither collapse nor contraction of the defect, and the dermal repair tissue was considerably thicker and more organized. By 7 days, complete re-epithelialization of the HUCPVC wounds was observed whilst in the controls re-epithelialization was limited to the wound margins. Wound strength was significantly increased in the HUCPVC treatment group by 3 and 7 days but no statistical difference was seen at 10 days. We conclude that HUCPVCs accelerate early wound healing in full thickness skin defects and thus represent a putative source of human MSCs for use in dermal tissue engineering.

### Introduction

The poor healing of full thickness skin wounds remains a significant clinical problem. Currently available treatments do not result in optimal healing, in part, due to an inability to fully restore the structure and function, of the dermis. The extracellular matrix (ECM) of the dermis, formed principally by fibroblasts and containing a rich vasculature, provides a structural framework to support the epidermis. As such, dermal tissue engineering strategies have revolved around use of fibroblast-like cells from a variety of sources including autologous dermis, allogeneic foreskin and both autologous and allogeneic bone marrow.<sup>1,2</sup> Specifically, human bone marrow-derived mesenchymal stem cells (hBM-MSC) have been employed for both dermal tissue engineering in murine models<sup>3</sup> and for clinical treatment of cutaneous wounds by either direct<sup>4</sup> or fibrin spray<sup>5</sup> delivery. Allogeneic strategies are possible because MSC are both immunoprivileged and can be easily cryopreserved, which presents the opportunity of stockpiling MSC as therapeutics. However, the numbers of MSC rapidly decrease in bone marrow,<sup>6</sup> and their procurement is invasive; thus other sources of MSC are being explored. Indeed, it is now

generally accepted that hBM-MSC are perivascular cells<sup>7</sup> and also that MSC can be ubiquitously found in all tissues of the body,<sup>8</sup> resident in the perivascular niche.<sup>8</sup>

We have previously described a rich source of adult MSC obtained from the perivascular tissue of the human umbilical cord.<sup>10,11</sup> Human umbilical cord perivascular cells (HUCPVC) have been recognized by others as distinct from cells in the bulk of Wharton's Jelly,<sup>12,13</sup> and exceed the minimum criteria established by the International Society for Cell Therapy,<sup>14</sup> for mesenchymal stromal cells (also MSC). Independent *in vitro* studies have shown that HUCPVC demonstrate similar phenotypic characteristics to hBM-MSC with a significantly greater colony forming unit fibroblast (CFU-F) frequency than hBM-MSC<sup>15</sup> and can reduce activation and proliferation of alloreactive lymphocytes.<sup>16</sup> Given their MSC phenotype and facile procurement, we hypothesized that HUCPVC may constitute an alternative source of cells for dermal wound healing as they avoid the inherent sourcing limitations posed by hBM-MSC. Thus, the purpose of the present study was to determine whether fluorescently stained HUCPVC delivered in fibrin into skin defects in immune-compromised mice would contribute to dermal healing.

\*Correspondence to: J.E. Davies; Email: [davies@ecf.utoronto.ca](mailto:davies@ecf.utoronto.ca)

Submitted: 03/19/10; Revised: 05/10/10; Accepted: 05/11/10

Previously published online: [www.landesbioscience.com/journals/organogenesis/article/12393](http://www.landesbioscience.com/journals/organogenesis/article/12393)

DOI: 10.4161/org6.4.12393

## Results

All animals, both Balb/c nude mice and Wistar rats, recovered uneventfully from surgery.

After 7 days, marked differences were evident between the appearance of the control and HUCPVC treated 4 mm diameter wounds. In the former, the original circular wound outline was still clearly visible with a central eschar (Fig. 1A), while the latter showed almost complete healing, the original wound margins were not appreciable and the eschar was barely visible (Fig. 1B). Qualitatively, there was an increased angiogenic response in the HUCPVC-treated wounds when compared to control (Compare Fig. 1C and D). In fact, histological differences were already evident at 3 days where the fibrin controls failed to provide a template for host cellular ingrowth, which resulted in a very thin dermal repair and considerable contraction of the defect (Fig. 2A). In contrast, HUCPVCs could be easily visualized within the fibrin matrix, which did not collapse and thus resulted in no apparent contraction of the wound site (Fig. 2B). Fluorescence microscopy confirmed the presence of HUCPVCs encapsulated within the fibrin matrix, and HUCPVCs were observed migrating away from the fibrin and in direct contact with host-derived cells both in the epidermis and dermis (not shown). In HUCPVC treatment groups, re-epithelialization occurred by keratinocyte migration, over the fibrin, from the lateral wound margins. These migrating cells were negative for PKH67.

Histologically, by 7 days, the granulation tissue in the dermis was considerably thicker in the HUCPVC laden constructs than in contralateral controls. HUCPVCs could be clearly identified migrating away from the inferior border of the fibrin matrix and interacting with cells of the host dermis. Complete re-epithelialisation of wounds was observed in all HUCPVC treated defects whilst this was not observed in contralateral controls in which the epithelial tissue remained at the wound margins (Fig. 3A). At the lateral margins of the defect at 7 days, migrating HUCPVCs were identified in direct contact with the ingrowing host-derived epithelial cells. Rete ridge formation was observed in the HUCPVC treated wounds while the epithelial-dermal junction in the controls was comparatively poorly developed. PKH-67 labeled cells were also clearly identified resident in the granulation tissue of the dermis with a reduced fluorescent signal as compared to 3 days (Fig. 3D). No adnexal structures were observed in the repair tissue in either

control or treatment groups.

**In vivo HUCPVC survival and ex vivo proliferation.** Digestion of the wound site yielded an average of  $(0.76 \pm 0.26) \times 10^6$  cells from control defects and an average of  $(1.23 \pm 0.02) \times 10^6$  cells from the HUCPVC-laden defects. Cell viability ranged from 75.4 to 85.5% ( $n = 3$ ). Fluorescence microscopic observation of these cells demonstrated an absence of PKH-67-stained

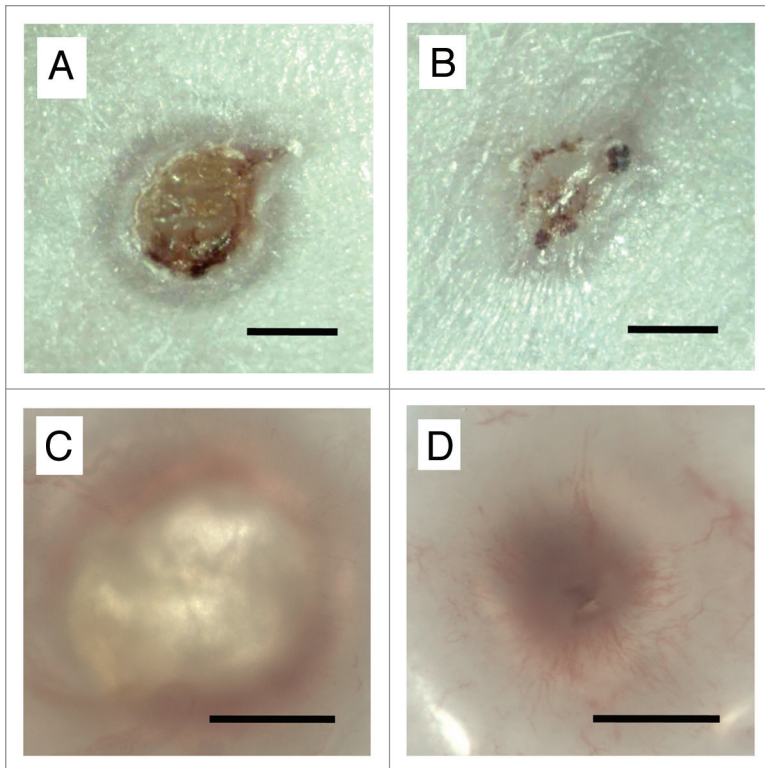


**Figure 1.** Photomicrographs of (A and C) control and (B and D) HUCPVC-containing wounds at 7 days. Note in (A) the size of the original circular wound and with annular repair and central eschar. (B) The HUCPVC-treated wound shows more advanced repair. (C and D) Wounds viewed by transillumination show little vascularization in the control (C) but marked radial arrays of blood vessels in the HUCPVC treated wound (D). Bars = 2 mm.

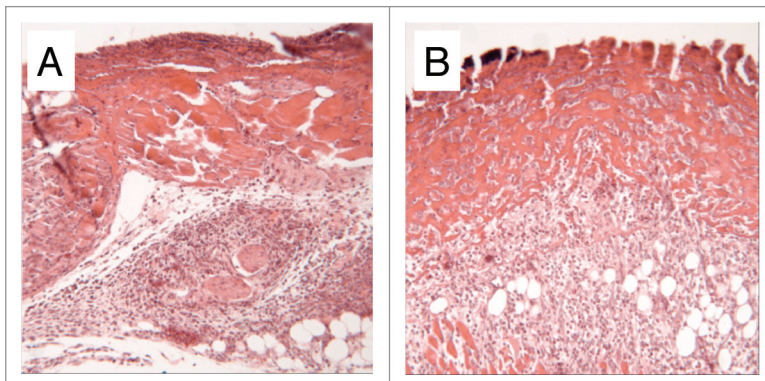


**Figure 2.** Sections of 4 mm diameter defects at 3 days. (A) Fibrin control, note poorly organized dermis. (B) HUCPVC in fibrin, note the obvious presence of cells within the fibrin and the resulting maintenance of dermal thickness. Field width for each image: 858  $\mu\text{m}$ .

To confirm the survival of HUCPVC in this model, we digested biopsy specimens of the wounds and cultured the harvested cells; while to confirm the ability of HUCPVC to produce a collagenous ECM *in vivo* we also inoculated them into diffusion chambers that were implanted in the peritoneal cavity of Wistar rats.



cells in digests from the control sites (Fig. 4A), but revealed the presence of PKH-67-stained HUCPVCs in digests obtained from treatment defects (Fig. 4B). Ki67 positive nuclei were co-localized to PKH67 positive cells indicating the continued ability of the human cells, recovered from wound digests, to proliferate in culture (Fig. 4C).

**Mechanical testing, 8 mm defects.** At 3 days post-operative, in all six animals, the HUCPVC containing wound showed an increase in mean tensile strength as compared to the contralateral control. The overall mean tensile strength of the treatment group was  $53.7 \pm 12.6$  kPa, which was approximately 4 times greater than that of the control group ( $12.7 \pm 13.9$  kPa). Statistical analysis using the non-parametric Wilcoxon Matched-Pairs Signed-Rank Test revealed a significant increase in wound tensile strength in HUCPVC-laden defects as compared with controls as this time point ( $p < 0.031$ ). Similarly, at 7 days post-operative, in all six animals, the HUCPVC containing wounds showed an increase in mean tensile strength as compared to the contralateral controls (Fig. 5). The overall mean tensile strength of the treatment group ( $218.2 \pm 20.4$  kPa) was found to be 2.7 times greater than that of the control group ( $80.5 \pm 47.2$  kPa), a significant increase in wound tensile strength (WTS) in HUCPVC-laden defects as compared with controls ( $p < 0.031$ ). By 10 days post-operative, the overall mean tensile strength of the treatment group ( $281.9 \pm 62.6$  kPa) was still higher than that of the control group ( $250.4 \pm 87.5$  kPa), although this difference was no longer significant ( $p > 0.6$ ). Time course analysis of all groups demonstrated an accelerated rate of gain of WTS to 7 days in the HUCPVC-treated groups, but neither control nor treatment group attained the values of normal skin within the timeframe of our experiment (Fig. 6).

**Synthetic activity of HUCPVC in vivo.** SEM analysis of 10 mm diameter diffusion chambers containing  $0.5 \times 10^6$  HUCPVCs revealed extensive fibrous extracellular matrix formation at both 4 and 7 days post-operative. This ECM stained positive for picrorisurid and eosin (not shown). The amount and density of this matrix appeared to increase from 4 to 7 days (Fig. 7A and B). Freeze fracture of 4mm defects at 7 days demonstrated a more organized dermal ECM than contralateral controls (Fig. 7C and D).

## Discussion

We sought to determine whether HUCPVCs would contribute to dermal healing following their delivery to full thickness defects in murine skin. Compared to fibrin-only controls, introduction of HUCPVCs within fibrin sealant provided superior reconstitution of the dermis and allowed rapid re-epithelialization of the wounds. These findings are in accordance with others who report that the use of BM-MSC in treatment of excisional skin wounds in rodents improves the rate at which the defect heals.

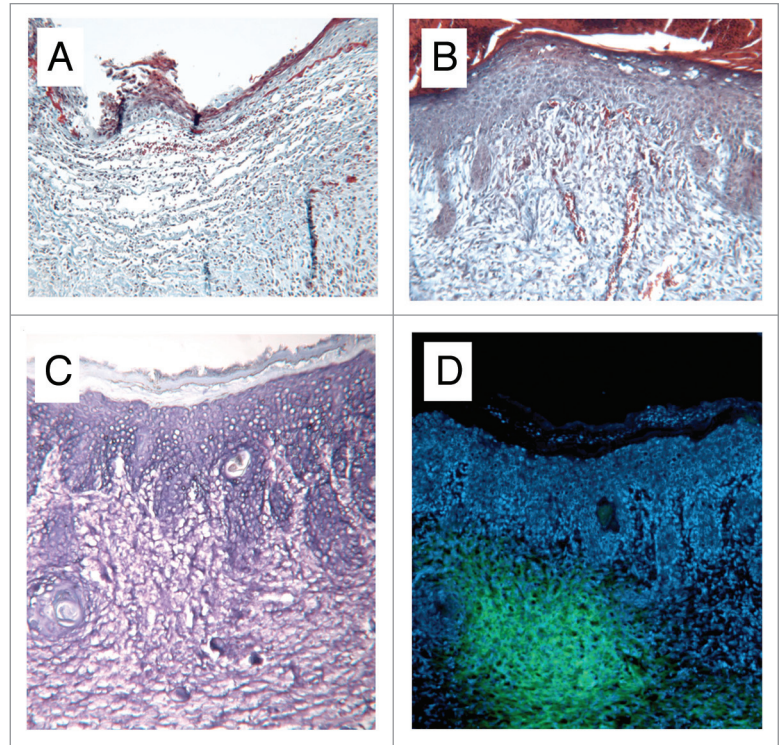


**Figure 3.** Photomicrographs of cryosections of (A) control and (B) HUCPVC-treated defects at 7 days showing incomplete re-epithelialization in the control and complete re-epithelialization in the HUCPVC specimen. Note the prominent microvasculature in (B). (C and D) show a pair of serial cryosections of a HUCPVC-treated defect at 7 days. (C) stained with Toluidine blue, shows the general tissue morphology with rete ridge formation, while the epifluorescent image in (D) shows the localization of the HUCPVC in the dermis. Field widths: (A and B) 2,144  $\mu\text{m}$ , (C and D) 858  $\mu\text{m}$ .

Wu et al.<sup>17</sup> observed thicker, more cellular and highly vascular granulation tissue in BM-MSC-treated defects as compared to controls at 7 and 14 days postoperative. McFarlin et al.<sup>18</sup> also demonstrated that linear incisional abdominal wounds in rats injected intradermally with allogenic BM-MSC demonstrated increased granulation tissue formation. This granulation tissue was observed to be more organized and collagenous in nature than PBS only controls at 7 days post-operative. The observation of rete ridges in the HUCPVC treated defects at 7 days suggests a strong dermal-epidermal junction in the HUCPVC group as these ridges are associated with the maturity of the attachment between the epidermis and dermis.<sup>19</sup> HUCPVCs were found exclusively in the dermal tissues and we found no evidence that the introduced HUCPVCs contributed to epithelial structures or adnexal structures of the dermis. This is in contrast to Wu et al.<sup>12</sup> who identified cytokeratin expressing BM-MSC in the epidermis, dermal-epidermal junction as well as in developing skin appendages. Furthermore, Nakagawa et al.<sup>3</sup> detected human cytokeratin expression in rat excisional wounds treated with hBM-MSCs. We postulate that HUCPVCs may play both a structural role—maintaining the dermis, preventing wound collapse—and a paracrine role; eliciting increased vascularization and epithelial overgrowth. The increased vascularity of the HUCPVC-treated

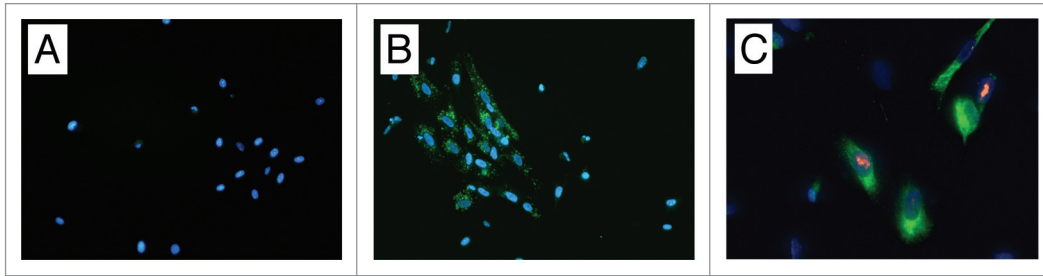


**Figure 4.** Fluorescence microscopy of cultures obtained from wound digests. (A) Murine cells derived from digestion of control defects, no presence of PKH67. (B) Populations of PKH-67-stained HUCPVCs were identified alongside murine-derived cells following digestion of treatment defects. Intact DAPI-stained nuclei indicate viable cells. (C) Immunocytochemical analysis for Ki-67 (red, visualized using Texas red) colocalized to DAPI-stained cell nuclei of PKH67-positive (green) HUCPVCs. Field widths: (A and B) 29  $\mu\text{m}$ , (C) 214  $\mu\text{m}$ .

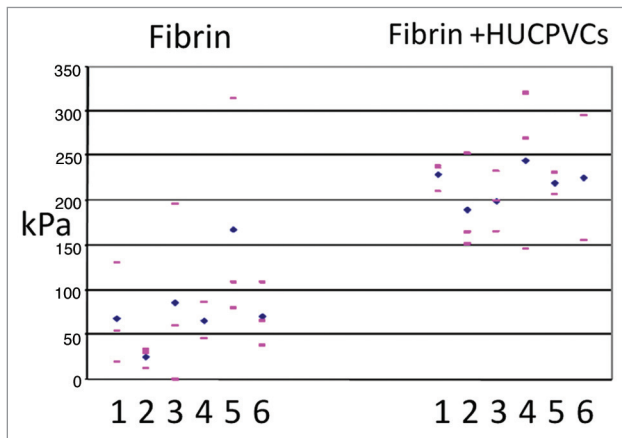


**Figure 5.** Individual wound tensile strength measurements of 8 mm diameter full thickness circular defects 7 days post-operative. For each animal (numbered 1–6) pink bars represent single tensile measurements and blue diamonds represent mean wound tensile strength.

wounds, compared to controls, corroborates the findings of Wu et al.<sup>12</sup> and Hung et al.<sup>20</sup> who reported the angiogenic effects of human MSCs.

We have recently shown, using single cell seeding clonal assays, that HUCPVCs exhibit both self-renewal and multi-differentiation potential, and thus possess the hallmark characteristics of stem cells.<sup>7</sup> However, we also showed that not only is this population heterogeneous, with stem cells exhibiting differing capacities for multilineage differentiation potential, but that the default (terminal) lineage was fibroblastic. In the present work, we hypothesized that a culture expanded, and thus predominantly fibroblastic HUCPVC population, could increase the rate of dermal healing by directly synthesizing new dermal ECM. To determine if it was indeed possible for HUCPVCs to play a direct synthetic role in dermal healing we sought to establish both their viability post transplantation and their synthetic activity in an alternative *in vivo* model. Thus, we showed that HUCPVCs, like BM derived cells, synthesize fibrous ECM *in vivo* following implantation in diffusion chambers in the peritoneal cavity of normal rats, which suggests that these cells retain the capacity to contribute to the ECM formation during healing. Furthermore, our labeling with PKH67 suggested that HUCPVCs were proliferating in

the wound site, since PKH67 is a membrane-bound dye and, as the cell divides, the membrane is split between daughter cells, thereby decreasing fluorescence intensity over time<sup>21</sup> as witnessed by the more diffuse fluorescence of PKH67 at 7 days compared to that at 3 days. Indeed, this was confirmed by the more rigorous determination of proliferation using Ki67 localization within the nuclei of PKH67-stained HUCPVCs digested from the wound sites, which provides robust evidence of the continuing *in vitro* proliferative capacity of these cells following *in vivo* implantation.

In cell-based regenerative medicine applications, choice of cell delivery vehicle is an important consideration. We selected fibrin sealant as it is a clinically relevant method to deliver cells to dermal wounds.<sup>5</sup> In addition, fibrin is a substrate that acts as a provisional matrix through which cells migrate, in normal wound healing, to populate the wound site.<sup>22</sup> It has previously been shown that the encapsulation of mesenchymal cells in Tisseel<sup>®</sup> requires dilution of both fibrin and thrombin components. Specifically, Cox et al.<sup>23</sup> found formulations using higher levels of fibrinogen (34–50 mg/ml) adversely affected the proliferation of fibroblasts. These cells proliferated well at 17 mg/ml of fibrinogen and 167 I.U. of thrombin. Using BM-MSCs, Ho et al.<sup>24</sup> confirmed this observation; citing lower concentrations of fibrinogen (5 mg/ml) were preferable to facilitate cell proliferation. Using these data as a guide we evaluated various fibrin and thrombin concentrations and found that 11.25 mg/mL of fibrinogen and 25 I.U. units of thrombin provided adequate mixing time at surgery (polymerization in approximately 10–15 seconds). In addition, this provided sufficient consistency of the fibrin gel, enabling it to remain in the wound site prior to placement of the semi-occlusive dressing.

HUCPVC-treated defects exhibited significantly higher WTS than controls and similar results have been shown with BM-MSC. In an incisional wound model, McFarlin et al.<sup>13</sup> demonstrated a significant increase in WTS of MSC treated rats at 7 days post-operative. However, WTS is not only a function of tissue quantity but also tissue organization. Therefore we observed collagen orientation of freeze-fractured wound sites using SEM. We observed thick, organized collagen fibers in HUCPVC-laden defects whereas in the controls, the collagenous ECM appeared more irregularly arranged. Doillon et al.<sup>25</sup> have demonstrated that WTS is directly related to collagen bundle arrangement. Therefore, it is likely that the increase in collagen organization

of HUCPVC-laden defects played a role in the increased WTS observed at 7 days. Time course analysis of WTS showed an increased rate of gain of tensile strength in HUCPVC-laden defects compared to controls from 3 to 7 days post-operative. This suggests an acceleration of healing events, particularly ECM formation, in HUCPVC-laden defects as compared to controls. Interestingly, a decreased variability was associated with WTS measurement of HUCVPC containing defects as compared to fibrin only controls at all time points, demonstrating that healing events such as granulation tissue formation occurred more evenly distributed in the wound site of these samples whereas in controls healing most likely occurs at the wound edges. By 10 days however, control wounds appeared as strong as the treatment defects.

As recently reviewed by Fu and Li,<sup>26</sup> there are many issues still to be addressed with respect to the use of MSCs for skin regeneration, not least of which are the concerns that adnexal structures are generally not found in the reconstituted epithelium, although the work of Sasaki et al.<sup>27</sup> may indicate the possibility of trans-germ line differentiation of MSCs in this regard. But Fu and Li<sup>21</sup> also caution that it will only be when adult mesenchymal stem cells of sufficient purity and quantity are readily available that such problems will be more readily investigated. Indeed, the molecular signaling events controlling the epithelial niche are now being deconvoluted,<sup>28,29</sup> and given suitable MSC populations, it is conceivable that the mesenchymal/epithelial interactions underlying adnexal development could soon be addressed. Given the high frequency of MSCs in HUCPVC populations, which we have shown herein can accelerate dermal wound healing and their demonstrated robust expansion from single cells,<sup>7</sup> we believe that this rich human mesenchymal stem cell source could find utility in addressing some of the important outstanding questions in skin regeneration.

## Materials and Methods

**Isolation of HUCPVC.** Umbilical cords were obtained from full-term, consenting donors undergoing caesarean section at Women's College Hospital, Toronto. HUCPVCs were extracted as previously described.<sup>6</sup> The cells were cultured in alpha minimal essential medium (Invitrogen, Canada) supplemented with 10% fetal calf serum (Hyclone, Canada), 10% penicillin/gentamycin (Sigma-Aldrich, Canada) and were expanded for two passages to yield sufficient cells for transplantation.

**Cell labeling and fibrin delivery.** For tracking *in vivo*, cells were stained with PKH67 membrane dye (Sigma-Aldrich) according to manufacturers instructions. Prior to transplantation, viability of cells was assessed using a ViCell (Beckman Coulter, Canada).

For delivery into 4 mm diameter wounds, HUCPVCs were suspended in Tisseel® Fibrin Sealant (Baxter, Canada). Immediately prior to surgery, 25  $\mu$ L of phosphate-buffered saline (PBS), either alone or containing  $1 \times 10^6$  PKH67-labeled HUCPVC, was mixed with 100  $\mu$ L of fibrinogen/aprotinin diluted in PBS to 18 mg/mL<sup>-1</sup>. The fibrinogen component was mixed with 125  $\mu$ L of 50 I.U. of thrombin, yielding control (fibrin only) and treatment

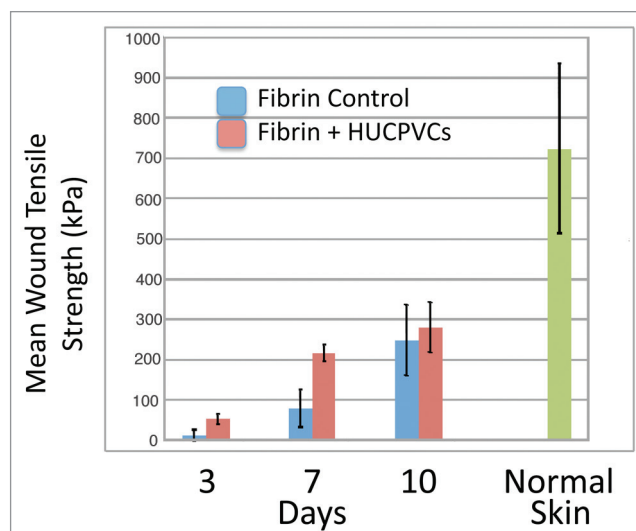


**Figure 6.** Mean wound tensile strength (kPa) of 8 mm diameter full thickness circular defects at 3, 7 and 10 days postoperative compared with normal skin. Bars represent standard deviations for each value.

(fibrin + HUCPVCs) groups. Following the polymerization of the fibrin, gels were applied directly to the wound site.

For delivery into 8 mm diameter wounds the concentrations of fibrinogen/aprotinin and thrombin remained the same, however 100  $\mu$ L of PBS either alone or containing  $4 \times 10^6$  PKH67-labeled HUCPVC was mixed with 400  $\mu$ L of fibrinogen. This was then mixed with 500  $\mu$ L of thrombin yielding control (fibrin only) and treatment (fibrin + HUCPVCs) groups.

**Skin wound model.** The following protocol was approved by the Animal Care Committee of Princess Margaret Hospital (PMH), Toronto. Under halothane anaesthesia, bilateral, full thickness defects were created in the dorsum of female Balb/c nude mice using a biopsy punch (Acuderm®, FL). Defects were either 4 mm ( $n = 12$ ) or 8 mm ( $n = 16$ ) in diameter, mirrored in the cranial-caudal axis and included removal of panniculus carnosus. 8 mm defects were used solely for mechanical testing. One defect received only the fibrin gel and served as internal control while the contralateral defect received HUCPVC in a fibrin gel. Wounds were covered with Tegaderm™ non-occlusive dressing (3 M, MN). Post-operatively, animals received subcutaneous Temgesic (0.04 mg/kg<sup>-1</sup>). Animals were housed individually in the Animal Facility at the Ontario Cancer Institute, PMH and received sterilized food and water *ad libitum*. Four mm defect groups were left for 3 days ( $n = 3$ ), 5 days ( $n = 5$ ) or 7 days ( $n = 6$ ). Eight mm defect groups were left for 3 days ( $n = 6$ ), 7 days ( $n = 6$ ) or 10 days ( $n = 4$ ).

**Histological analysis, 4 mm diameter defects.** Following euthanasia, skin tissue around both control and treatment defects was excised, separated and fixed for 10 minutes in formalin. Samples were bisected through the circular wound site. Half was immediately frozen in liquid nitrogen in preparation for cryosectioning and SEM analysis. The other half remained in formalin overnight and was prepared for wax histology and stained with Haematoxylin and Eosin or Masson's Trichrome.



Serial cryosections taken from the bisected surface were counterstained with DAPI and evaluated by both brightfield and epifluorescence microscopy.

**Mechanical testing, 8 mm diameter defects.** Following euthanasia, a rectangular piece of skin surrounding both the control and experimental defects was removed allowing approximately 10 mm of skin cranial and caudal to the defect. Control and experimental defects were separated. Each wound was then cut into 2 mm strips through the defect so as to provide approximately 10 mm of normal skin on either side of the wound to place in the grips of the testing machine. Strips were placed in PBS and immediately taken for testing. An INSTRON MTS system with 2.5 g load cell was used to load the skin samples in tension. The ends of the skin strips were secured into the grips of the MTS that had been covered with tape to improve anchorage. Samples were distracted at a rate of 20 mm/min until failure. To assess the statistical significance of the difference in wound tensile strength between either the treatment or control groups and normal skin, a Welch's t test was used. It was assumed that the samples had a normal distribution, but that any two groups had unequal variance. In all cases,  $p < 0.05$  was taken to be significant.

**In vivo HUCPVC survival and ex vivo proliferation.** Tissue was harvested from 4 mm defects ( $n = 3$ ) at 5 days. Control and HUCPVC-treated wounds were subjected to enzymatic digestion as described by Wilson et al. (2002).<sup>30</sup> Following euthanasia, 8 mm biopsy punches were used to remove the tissue surrounding the 4 mm diameter wound. Biopsy samples were diced into 2 mm pieces and incubated overnight at 4°C in a solution comprising Hanks Balanced Salt Solution (Gibco, Invitrogen, Canada), 1 mg/ml dispase I (Roche Molecular Biochemicals, IN), 3% heat-inactivated FBS and 10 mg/ml gentamycin (Sigma, St. Louis, MO). The next day the samples were transferred to a solution comprising alpha MEM (Gibco, Invitrogen, Canada), 1 mg/ml hyaluronidase (Sigma, St. Louis, MO), 1 mg/ml collagenase (Sigma, St. Louis, MO), 150 U/ml DNase (Arcturus, CA) and 5 mg/ml gentamycin (Sigma, St. Louis, MO). Solutions were placed at 37°C for 2 hrs after which they were forced through a 70 µm cell strainer (Sigma, St. Louis, MO), centrifuged, washed in PBS and plated directly onto sterile glass coverslips in the bottom of a 6-well plate (Beckton Dickinson Labware, Franklin Lakes, NJ). Cultures were analyzed by phase contrast and fluorescence microscopy after 1 day in culture. Proliferation of HUCPVCs in culture was assessed by indirect immunocytochemical detection of Ki67 (Abcam, UK).

**Synthetic activity of HUCPVC within diffusion chambers in vivo.** Diffusion chambers, as previously described by Davies,<sup>31</sup> were used to assess the capacity of HUCPVCs to elaborate an extracellular matrix in vivo. Diffusion chamber kits were purchased from Millipore (Millipore, USA) and assembled according

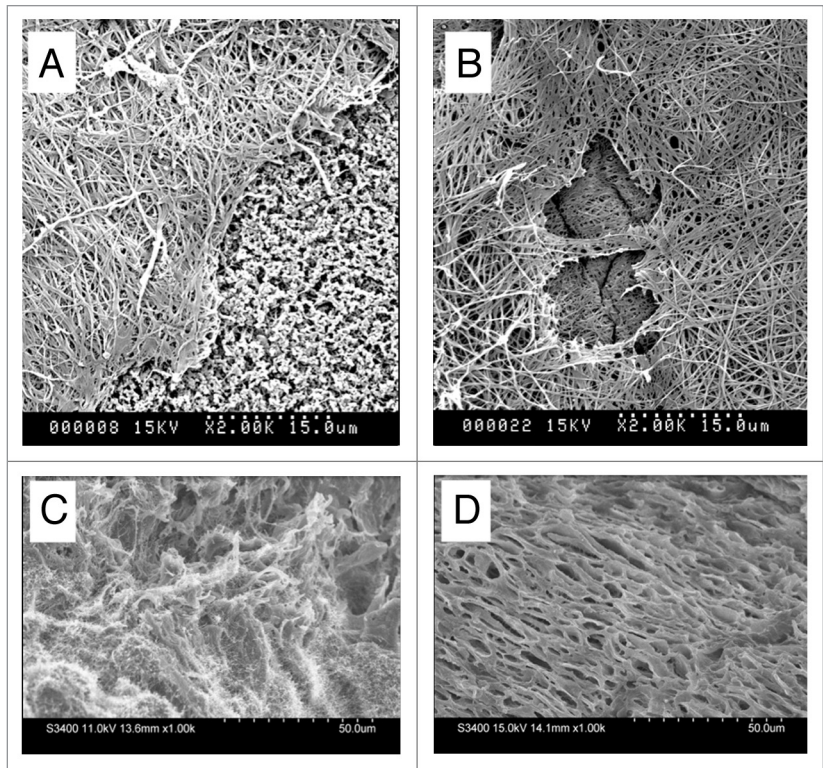


**Figure 7.** Scanning electron microscopy of (A and B) diffusion chambers innoculated with HUCPVCs and implanted intraperitoneally in rats for 4 and 7 days respectively. A fibrillar extracellular matrix is evident at both time points. The exposed cellulose acetate filter (f) seen at 4 days but not at 7 days suggests continued HUCPVC synthetic activity in vivo to 7 days. (C and D) Freeze fractured 4 mm diameter full thickness circular defects at 7 days post-operative (C) from fibrin-only control wound; (D) from fibrin + HUCPVC wound. Note, in the latter, the organized stratified appearance of the ECM.

to manufacturers instructions. Chambers were made by cementing two 0.45 µm pore size filters (Millipore, USA) to either side of a circular Plexiglas™ ring. Prior to inoculation with HUCPVCs, diffusion chambers were gamma-sterilized (2.5 MRad).

Culture expanded HUCPVC's (P4) were trypsinized, counted and resuspended in order to obtain 50 µl aliquots of a cell suspension containing  $0.5 \times 10^6$  cells. Cells were pipetted directly into sterile diffusion chambers via the lateral access port. The access port was then sealed using sterile nylon cord and acrylic cement (Millipore, USA). Inoculated chambers and empty control chambers were stored in 12-well tissue culture plates containing 3 mls of SM and incubated at 37°C overnight ready for surgery the following day.

**Intraperitoneal implantation of diffusion chambers.** The following protocol was approved by the local Animal Care Committee at the Faculty of Dentistry, University of Toronto, Canada. 225–250 g male Wistar rats were anesthetized using isoflurane. The abdomen of the animals was shaved and swabbed with 70% ethanol and povidone iodine. A midline incision was created along the lower abdominal skin and underlying muscle wall using a scalpel. A loop of small intestine was withdrawn from the peritoneal cavity and placed on sterile, saline-soaked gauze. Previously prepared diffusion chambers

(empty or containing HUCPVCs) were wrapped in the omentum. The bowel and chamber were then returned to the peritoneal cavity. The abdominal wall was closed with resorbable sutures (Vicryl) and the skin was then closed with silk sutures (Ethicon, J&J, USA). Rats were sacrificed at either 4 or 7 days post-operative and diffusion chambers removed and fixed in in Karnovsky's fixative (5% glutaraldehyde, 4% paraformaldehyde in 0.08 M sodium phosphate Buffer) and stored at 4°C for at least 24 hours. Samples were then dehydrated in ascending alcohols and critically point dried (Tousimis, Autosamdri 850B,

Rockville, MD). Samples were coated with a 20 nm thick layer of gold via a Sputter Coater (Polaron, Quorum Technologies, UK) and examined under the SEM (Hitachi S570, Japan).

#### Acknowledgements

The authors would like to thank Patralika Chattopadhyay for preparation of paraffin sections, Jian Wang (Faculty of Dentistry) for mechanical testing and Susan Carter (Faculty of Dentistry) for animal surgeries and an Ontario Research and Development Challenge Fund (ORDCF) grant to J.E.D.

#### References

1. Wong T, McGrath JA, Navsaria H. The role of fibroblasts in tissue engineering and regeneration. *Br J Dermatol* 2007; 156:1149-55.
2. Nolte SV, Xu W, Rennekampff HO, Rodemann HP. Diversity of fibroblasts—A review on implications for skin tissue engineering. *Cells Tissues Organs* 2008; 153:29-36.
3. Nakagawa H, Akita S, Fukui M, Fujii T, Akino K. Human mesenchymal stem cells successfully improve skin-substitute wound healing. *Br J Dermatol* 2005; 153:29-36.
4. Badiavas EV, Falanga V. Treatment of chronic wounds with bone marrow-derived cells. *Arch Dermatol* 2003; 139:510-6.
5. Falanga V, Iwamoto S, Chartier M, Yufit T, Butmarc J, Kouttab N, et al. Autologous bone marrow-derived cultured mesenchymal stem cells delivered in a fibrin spray accelerate healing in murine and human cutaneous wounds. *Tissue Engineering* 2007; 13:1299-312.
6. Haynesworth SE, Goldberg VM, Caplan AL. Diminution of the number of mesenchymal stem cells as a cause for skeletal aging. In: Buckwalter JA, Goldberg VM, Woo SLY, Eds. *Musculoskeletal Soft-tissue Aging: Impact on Mobility* (section 1). Rosemont, IL: American Academy of Orthopaedic Surgeons 1994; 79-87.
7. Shi S, Gronthos S. Perivascular niche of postnatal mesenchymal stem cells in human bone marrow and dental pulp. *J Bone Miner Res* 2003; 18:696-704.
8. Crisan M, Yap S, Casteilla L, Chen CW, Corselli M, Park TS, et al. A perivascular origin for mesenchymal stem cells in multiple human organs. *Cell Stem Cell* 2008; 3:301-13.
9. Diaz-Flores L, Gutierrez R, Madrid JF, Varela H, Valladares F, Acosta E, et al. Pericytes. Morphofunction, interactions and pathology in a quiescent and activated mesenchymal cell niche. *Histol Histopathol* 2009; 24:909-69.
10. Sarugaser R, Lickorish D, Baksh D, Hosseini MM, Davies JE. Human umbilical cord perivascular (HUCPV) cells: a source of mesenchymal progenitors. *Stem Cells* 2005; 23:220-9.
11. Sarugaser R, Hanoun L, Keating A, Stanford WL, Davies JE. Human mesenchymal stem cells self-renew and differentiate according to a deterministic hierarchy. *PLoS One* 2009; 4:6498.
12. Can A, Karahuseynoglu S. Concise Review: Human umbilical cord stroma with regard to the source of fetus-derived stem cells. *Stem Cells* 2007; 25:2886-95.
13. Schugar RC, Chirieleison SM, Wescoe KE, Schmidt BT, Askew Y, Nance JJ, et al. High harvest yield, high expansion and phenotype stability of CD146 mesenchymal stromal cells from whole primitive human umbilical cord tissue. *J Biomed Biotechnol* 2009; 2009:789526.
14. Dominici M, Le Blanc K, Mueller I, Slaper-Cortenbach I, Marini F, Krause D, et al. Minimal criteria for defining multipotent mesenchymal stromal cells. The International Society for Cellular Therapy position statement. *Cytotherapy* 2006; 8:315-7.
15. Baksh D, Yao R, Tuan RS. Comparison of proliferative and multilineage differentiation potential of human mesenchymal stem cells derived from umbilical cord and bone marrow. *Stem Cells* 2007; 25:1384-92.
16. Ennis J, Gotherstrom C, Le Blanc K, Davies JE. In vitro immunologic properties of human umbilical cord perivascular cells. *Cytotherapy* 2008; 10:174-81.
17. Wu Y, Chen L, Scott PG, Tredget EE. Mesenchymal stem cells enhance wound healing through differentiation and angiogenesis. *Stem Cells* 2007; 25:2648-59.
18. McFarlin K, Gao X, Liu YB, Dulchavsky DS, Kwon D, Arbab AS, et al. Bone marrow-derived mesenchymal stromal cells accelerate wound healing in the rat. *Wound Repair Regen* 2006; 14:471-8.
19. van Zuijlen PP, Lamme EN, van Galen MJ, van Marle J, Kreis RW, Middlekoop E. Long-term results of a clinical trial on dermal substitution. A light microscopy and Fourier analysis based evaluation. *Burns* 2002; 28:151-60.
20. Hung SC, Pochampally RR, Chen SC, Hsu SC, Prockop DJ. Angiogenic effects of human multipotent stromal cell conditioned medium activate the PI3K-Akt pathway in hypoxic endothelial cells to inhibit apoptosis, increase survival and stimulate angiogenesis. *Stem Cells* 2007; 25:2363-70.
21. Rousselle C, Barbier M, Comte VV, Alcouffe C, Clement-Lacroix J, Chancel G, et al. Innocuousness and intracellular distribution of PKH67: a fluorescent probe for cell proliferation assessment. *In Vitro Cell Dev Biol Anim* 2001; 37:646-55.
22. Singer AJ, Clark RA. Cutaneous wound healing. *N Eng J Med* 1999; 341:738-46.
23. Cox S, Cole M, Tawil B. Behavior of human dermal fibroblasts in 3D fibrin clots: dependence on fibrinogen and thrombin concentration. *Tissue Eng* 2004; 10:942-54.
24. Ho W, Tawil B, Dunn JC, Wu BM. The behavior of human mesenchymal stem cells in 3D fibrin clot: dependence on fibrinogen concentration and clot structure. *Tissue Eng* 2006; 12:1587-95.
25. Doillon CJ, Dunn MG, Bender E, Silver FH. Collagen fiber formation in repair tissue: development of strength and toughness. *Coll Relat Res* 1985; 5:481-92.
26. Fu X and Li H. Mesenchymal stem cells and skin wound repair and regeneration: possibilities and questions. *Cell Tissue Res* 2009; 335:317-21.
27. Sasaki M, Abe R, Fujita Y, Ando S, Inokuma D, Shimizu H. Mesenchymal stem cells are recruited into wounded skin and contribute to wound repair by trans-differentiation into multiple skin cell type. *J Immunol* 2008; 180:2581-87.
28. Voog J, Jones DL. Stem cells and the niche: a dynamic duo. *Cell Stem Cell* 2010; 6:103-15.
29. Li L, Clevers H. Coexistence of quiescent and active adult stem cells in mammals. *Science* 2010; 327:542-5.
30. Wilson L, Fathke C, Isik F. Tissue dispersion and flow cytometry for the cellular analysis of wound healing. *Biotechniques* 2002; 32:548-51.
31. Davies JE. Human bone marrow cells synthesize collagen, in diffusion chambers, implanted into the normal rat. *Cell Biol Int Rep* 1987; 11:125-30.